# Ultrafast Photoinduced Intramolecular Charge Separation and Recombination Processes in the Oligothiophene−Substituted Benzene Dyads with an Amide Spacer

**ARTICLE** *in* THE JOURNAL OF PHYSICAL CHEMISTRY B · NOVEMBER 2005

Impact Factor: 3.3 · DOI: 10.1021/jp0534784 · Source: PubMed

THE JOURNAL OF PHYSICAL CHEMISTRY B



Article

# Ultrafast Photoinduced Intramolecular Charge Separation and Recombination Processes in the Oligothiophene-Substituted Benzene Dyads with an Amide Spacer

Yosuke Oseki, Mamoru Fujitsuka, Dae Won Cho, Akira Sugimoto, Sachiko Tojo, and Tetsuro Majima

*J. Phys. Chem. B*, **2005**, 109 (41), 19257-19262 • DOI: 10.1021/jp0534784

# Ultrafast Photoinduced Intramolecular Charge Separation and Recombination Processes in the Oligothiophene-Substituted Benzene Dyads with an Amide Spacer

**Yosuke Oseki, Mamoru Fujitsuka, Dae Won Cho, Akira Sugimoto, Sachiko Tojo, and Tetsuro Majima***

*The Institute of Scientific and Industrial Research (SANKEN), Osaka University, Mihogaoka 8-1, Ibaraki, Osaka 567- 0047, Japan*

*Received: June 27, 2005; In Final Form: August 9, 2005*

Photoinduced intramolecular charge separation (CS) and recombination (CR) processes of the tetrathiophene-substituted benzene dyads with an amide spacer (4T−PhR, R = 4-H (**1**), 4-CN (**2**), 3,4-$(CN)_2$ (**3**), 4-$NO_2$ (**4**), 3,5-$(NO_2)_2$ (**5**)) in solvents of different polarities were investigated using various fast spectroscopies. It was revealed that the CS rates depend on the ability of the acceptor and solvent polarity. Ultrafast CS with the rate of $5 \times 10^{12}$ $s^{-1}$ was revealed for **5** in PhCN and MeCN. The ultrafast CS can be attributed to the large electronic coupling matrix element between the donor and the acceptor despite the relative long donor−acceptor distance. The existence of the state with large electron density on the spacer between $^1$4T*−PhR and LUMO should facilitate the CS process in the present dyad system. It was also revealed that the CR rates in these dyads were rather fast because of the enhanced superexchange interaction through the amide spacer.

## Introduction

For years, oligo- and polythiophenes have been used in photovoltaic cells and organic semiconductor materials because of their ready accessibility, high $\pi$-conjugation, low oxidation potentials, and environmental stability.[1] The generation of charged species in the oligo- and polythiophene backbones is essential for their photoactive functions.[2] From this viewpoint, photoinduced charge separation (CS) and recombination (CR) processes are important processes to be clarified. The intramolecular CS and CR processes of the dyad systems containing oligothiophenes as an electron donor have been studied by various researchers.[3] As for the electron acceptors, various compounds such as fullerene[3a−c] and viologen dication[3d] have been employed. For example, the tetrathiophene−$C_{60}$ dyad has shown a CS with the rate constant ($k_{CS}$) of $2.4 \times 10^{10}$ $s^{-1}$ in THF. In the case of the octathiophene−methyl viologene dyad, the CS rate was estimated to be $9.9 \times 10^{10}$ $s^{-1}$.[3d] The CS rates of the octa- and dodecathiophene−$C_{60}$ dyads in a cluster were $>10^{12}$ $s^{-1}$.[3c] Moreover, the triad systems have also been studied.[4] Construction of the dyad system with a rather fast CS rate seems to be possible for these oligothiophene−acceptor dyad systems. However, systematic study optimizing the CS rate of these oligothiophene dyads by changing the electron-accepting ability of the acceptor has not yet been reported.[5]

Fast intramolecular CS is important in view of the optimization of the artificial light-energy conversion and the design of molecular devices such as molecular switches and logic gates, in which an ultrafast response is essential.[6] To realize the ultrafast CS in the dyad systems, the following two factors should be important: (1) Based on the Marcus theory, the Gibbs free energy change of the CS ($\Delta G_{CS}$) should be adjusted to the reorganization energy in order to realize the CS in the Marcus top region. (2) The spacer between the donor and the acceptor should be properly selected in order to realize a larger electronic coupling matrix element in the CS theory.[7]

In the present paper, we report ultrafast intramolecular CS processes in the systematically designed tetrathiophene-substituted benzene (4T−PhR, R = 4-H (**1**), 4-CN (**2**), 3,4-$(CN)_2$ (**3**), 4-$NO_2$ (**4**), 3,5-$(NO_2)_2$ (**5**)) dyads linked with an amide spacer (Figure 1) in toluene (Tol), anisole (ANS), tetrahydrofuran (THF), benzonitrile (PhCN), and acetonitrile (MeCN). The amide spacer was used to enhance the coupling between the donor and acceptor. The amide spacer is also beneficial for attaining a rigid structure of the dyads.[8] An extremely fast CS in the subpicosecond region was observed in the present dyads.

## Results and Discussion

**Molecular Orbital Calculation.** Figure 2 shows the optimized structures and electron densities of the highest occupied molecular orbital (HOMO, (A)), lowest unoccupied molecular orbital (LUMO, (B)), and second unoccupied molecular orbital (LUMO+1, (C)) of **5** as a representative compound. For simplicity, the hexyl substituents were reduced to ethyl groups. Except for a thiophene ring at the terminal end, the other part retains a planar structure. The electron density of the HOMO was delocalized on the tetrathiophene moiety. It should be stressed that a slight density was also distributed on the amide spacer, indicating a slightly enlarged $\pi$-conjugation in the dyad. The electron density of the LUMO was localized on the dinitrobenzene moiety. It is predicted that the formation of the CS state is possible upon excitation. On the other hand, the electron distribution of the LUMO+1 was confirmed on the amide spacer as well as on the dinitrobenzene and thiophene ring. The energy difference between the LUMO and LUMO+1 was estimated to be 0.30 eV. The state corresponding to the LUMO of tetrathiophene was LUMO+2 of the present dyad. The LUMO+2 was 0.26 eV higher than the LUMO+1. Therefore, after excitation of the tetrathiophene moiety of the dyad, the CS state will be generated through the mechanism

* Author to whom correspondence may be sent. E-mail: majima@sanken.osaka-u.ac.jp.

10.1021/jp0534784 CCC: $30.25 
Published on Web 09/28/2005

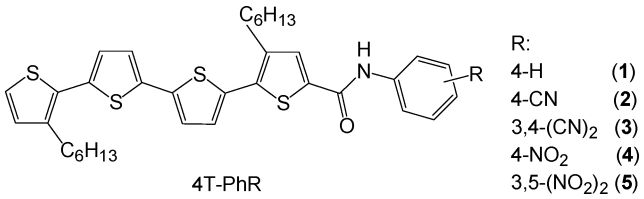


**Figure 1.** Structures of the dyads.

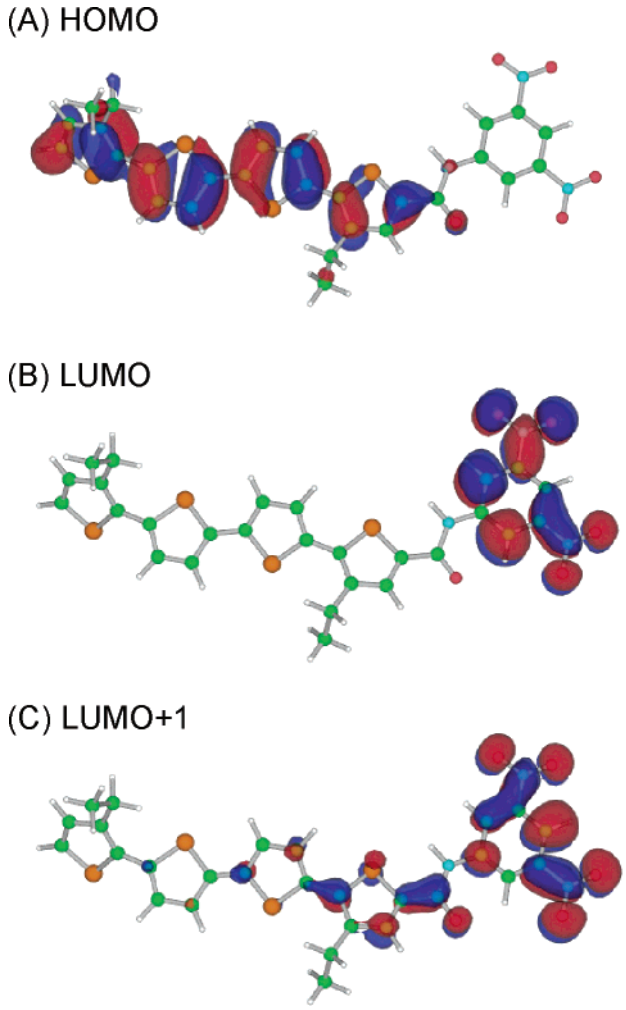


**Figure 2.** Optimized structures and electron densities of the HOMO (A), LUMO (B), and LUMO+1 (C) of **5** calculated at the B3LYP/6-31G(d) level, using ethyl groups instead of hexyl groups.

including the contribution of amide spacer.[9] Thus, the fast CS is expected for **5**. In cases **1** and **2**, the electron density of LUMO is on the tetrathiophene and spacer (see Supporting Information), suggesting absence of the CS upon excitation. As for **3** and **4**, the MO patterns were intermediate between **1** and **5**.

**Steady-State Absorption and Fluorescence.** Figure 3 shows the steady-state absorption and fluorescence spectra of the dyads in Tol. The absorption peak positions ($\lambda_{abs}$) of the dyads in various solvents are summarized in Table 1 and Table S1 (see Supporting Information). The absorption peak of these dyads shifted to a longer wavelength compared to that of tetrathiophene (380 nm, typically),[3a] indicating an extended $\pi$-conjugation, as suggested by the molecular orbital calculations. The absorption peak of the dyads slightly shifted, depending on the solvent. Since the peak positions are not in the order of solvent polarity, the interaction between the donor and acceptor, such as charge transfer, is not responsible for the present spectral shift. Since

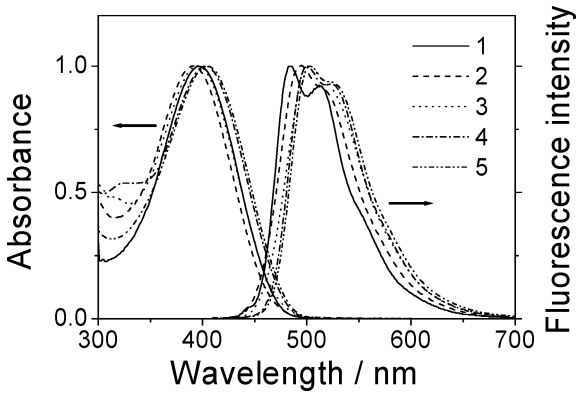


**Figure 3.** Normalized absorption and fluorescence spectra of the dyads in Tol.

**TABLE 1: Photophysical Properties of 4 and 5**

| cmpd | solvent | $\lambda_{abs}$ / nm | $\lambda_{fl}$ / nm | $\phi_{fl}$[a] | $\tau_{fl}$ / ps | $\phi_T$[b] | $\tau_T$ / $\mu$s |
|---|---|---|---|---|---|---|---|
| **4** | Tol | 403 | 500 | 0.12 | 490 | 0.38 | 28 |
| | ANS | 407 | 520 | 0.07 | 300 | 0.23 | 30 |
| | THF | 400 | 514 | 0.04 | 250 | 0.22 | 32 |
| | PhCN | 410 | 518 | 0.004 | 6.0 | 0.10 | 48 |
| | MeCN | 399 | 511 | $<10^{-3}$ | 0.53 | 0.11 | 30 |
| **5** | Tol | 401 | 503 | 0.11 | 100, 1200[c] | 0.35 | 26 |
| | ANS | 408 | 500 | 0.002 | 4.0 | 0.05 | 35 |
| | THF | 407 | 501 | 0.001 | 0.83 | 0.05 | 37 |
| | PhCN | 413 | 510 | $<10^{-3}$ | 0.20 | 0.05 | 49 |
| | MeCN | 399 | 504 | $<10^{-3}$ | 0.20 | 0.04 | 31 |

[a] Using tetrathiophene as a reference. [b] Estimated by using $\epsilon_{T1}$ of **4** in benzene and using benzophenone as a reference. [c] The fluorescence time profile of **5** in Tol showed biphasic decay.

the solvent with a benzene ring tends to shift the peak position to a longer wavelength, the observed peak shift may come from the interaction with the aromatic ring of the solvent.

The fluorescence peak positions ($\lambda_{fl}$) and quantum yields ($\phi_{fl}$) of the dyads were also estimated, as summarized in Table 1 and Table S1, using tetrathiophene as a standard.[10] The significant fluorescence quenchings with increasing solvent polarity were observed for **4** and **5**, suggesting the CS processes from $^1$4T*−PhNO$_2$ and $^1$4T*−Ph(NO$_2$)$_2$, respectively. In the cases of **1**, **2**, and **3**, no significant change in the $\phi_{fl}$ was observed even when the solvent polarity increased, indicating the absence of the CS process in these dyads with acceptors having a lower electron-accepting ability.

**Fluorescence Lifetimes.** The fluorescence lifetimes ($\tau_{fl}$) of **4** were estimated to be 490, 300, 250, 6.0, and 0.53 ps in Tol, ANS, THF, PhCN, and MeCN, respectively (Table 1, Figure 4). The shorter $\tau_{fl}$ in the polar solvents supports the CS from $^1$4T*−PhNO$_2$. On the other hand, the $\tau_{fl}$ of **1**, **2**, and **3** did not depend on the solvent polarity (Table S1) and are the essentially the same as 4T.[10] Thus, no CS from $^1$4T*−PhR is concluded for **1**, **2**, and **3** in the various solvents. No CS is also concluded for **4** in Tol. The $\tau_{fl}$ of **5** in PhCN and MeCN showed the same value; therefore, it is considered that the CS processes of **5** in PhCN and MeCN are near the Marcus top region as will be discussed later.[5] In the case of **5** in Tol, a biphasic fluorescence decay was observed. This finding can be interpreted as evidence for the CS from $^1$4T*−Ph(NO$_2$)$_2$ to 4T$^{\bullet+}$−Ph(NO$_2$)$_2^{\bullet-}$ and thermally activated repopulation of $^1$4T*−Ph(NO$_2$)$_2$ from the CS state.[5a,b,11] The time constants of the fast and slow decay components were estimated to be 100 ps and 1.2 ns, respectively.

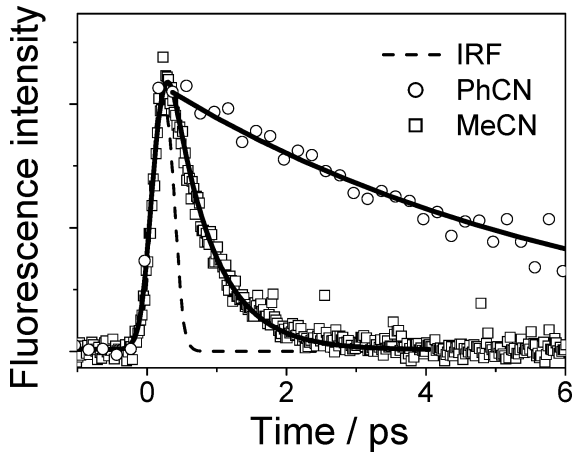


**Figure 4.** Fluorescence decay profiles of **4** in PhCN (○) and MeCN (□) . Bold lines are fitted curves. Dotted line is IRF. The fluorescence intensities are normalized.

**TABLE 2: Rate Constants, Yield, and Free Energy Changes for CS and CR of 4 and 5**

| cmpd | solvent | $\epsilon_{solvent}$[a] | $-\Delta G_{CS}$[b] / eV | $k_{CS}$[c] / $10^{12}$ $s^{-1}$ | $\phi_{CS}$[d] | $-\Delta G_{CR}$[b] / eV | $k_{CR}$ / $10^{10}$ $s^{-1}$ |
|---|---|---|---|---|---|---|---|
| **4** | Tol | 2.37 | −0.24 | 0 | 0 | 2.72 | 0 |
| | ANS | 4.33 | 0.18 | 0.0013 | 0.39 | 2.21 | − |
| | THF | 7.58 | 0.46 | 0.0020 | 0.50 | 1.95 | − |
| | PhCN | 25.2 | 0.70 | 0.17 | 0.99 | 1.70 | >3.3 |
| | MeCN | 35.94 | 0.86 | 1.7 | >0.99 | 1.57 | − |
| **5** | Tol | 2.37 | −0.01 | 0.0051 | − | 2.48 | 0.017 |
| | ANS | 4.33 | 0.51 | 0.25 | 0.99 | 1.97 | 1.4 |
| | THF | 7.58 | 0.77 | 1.2 | 0.99 | 1.71 | 2.7 |
| | PhCN | 25.2 | 0.97 | 5 | >0.99 | 1.46 | >3.3 |
| | MeCN | 35.94 | 1.03 | 5 | >0.99 | 1.43 | − |

[a] Data from ref 14. [b] $-\Delta G_{CR} = E_{ox} - E_{red} - \Delta G_S$, $-\Delta G_{CR} = \Delta E_{0-0} - (-\Delta G_{CR})$, $\Delta G_S = e^2/4\pi\epsilon_0[(1/(2r^+) + 1/(2r^-) - 1/R_{cc})/\epsilon_s - (1/(2r^+) + 1/(2r^-))/\epsilon_r]$ where $\Delta E_{0-0}$ refer to the lowest excited singlet state energy of 4T moiety; $E_{ox}$ and $E_{red}$ are the first oxidation potential of the donor and the first reduction potential of the acceptor in dichloromethane, respectively; $r^+$ and $r^-$ are radii of donor moiety (7.1 Å) and acceptor moiety (2.5 Å), respectively; $R_{cc}$ is the center-to-center distance between the two moieties (11.7 Å); and $\epsilon_s$ and $\epsilon_r$ are static dielectric constants of solvents used for the rate measurements and the redox-potential measurements. [c] Except for **5** in Tol (see text), $k_{CS} = (\tau_{fl})^{-1} - (\tau_0)^{-1}$, $\tau_0$ is the fluorescence lifetime of **4** in Tol. [d] $\phi_{CS} = k_{CS}/(\tau_{fl})^{-1}$.

For the other cases, the $k_{CS}$ and $\phi_{CS}$ of **4** and **5** were calculated by eqs 1 and 2, respectively,

$$k_{CS} = \tau_{fl}^{-1} - \tau_0^{-1} \quad (1)$$

$$\phi_{CS} = k_{CS}/\tau_{fl}^{-1} \quad (2)$$

where $\tau_0$ and $\tau_{fl}$ refer to the fluorescence lifetimes of the reference in Tol and the sample, respectively. The $k_{CS}$ and $\phi_{CS}$ values of **4** and **5** are summarized in Table 2.

**Picosecond Laser Flash Photolysis.** Figure 5 shows the transient absorption spectra of **5** in Tol (A, B) and ANS (C) during a 355-nm picosecond laser flash photolysis. In Tol, the absorption band attributable to $^1$4T*−Ph(NO$_2$)$_2$ was observed at 780 nm immediately after the laser irradiation. The absorption band at 780 nm showed a biexponential decay with the decay rates of $1.4 \times 10^{10}$ and $8.1 \times 10^8$ $s^{-1}$, which corresponded well to the respective fluorescence decay rates. With the initial decay of $^1$4T*−Ph(NO$_2$)$_2$, another sharp peak appeared at 690 nm (Figure 5A), which can be attributed to the radical cation of 4T[12] because it agrees with the radical cation of the dyads generated by pulse radiolysis.[13] Therefore, the appearance of

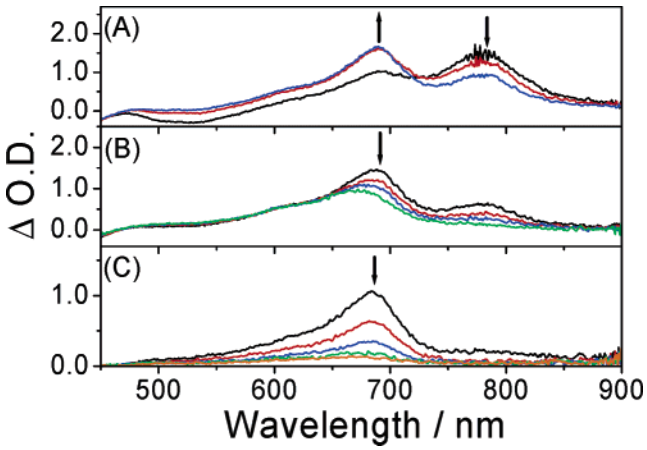


**Figure 5.** Transient absorption spectra of **5** in Tol at 50 (black), 100 (red), 200 (blue) ps (A), at 600 (black), 900 (red), 1400 (blue), and 2600 (green) ps (B), and in ANS at 30 (black), 100 (red), 150 (blue), 200 (green), and 400 (orange) ps (C) during a ps laser flash photolysis employing a ps Nd:YAG laser (355 nm, fwhm 30 ps, 4 mJ pulse$^{-1}$).

the absorption band at 690 nm is attributed to the CS process from $^1$4T*−Ph(NO$_2$)$_2$. From the decay of the absorption at 690 nm, the lifetime of the CS state ($\tau_{CS}$) was estimated to be 1.2 ns which corresponds to that of the slow decay component of $^1$4T*−Ph(NO$_2$)$_2$ (Figure 5B). The $k_{CS}$, $k_{CR}$, and rate constant of the back electron transfer from 4T$^{\bullet+}$−Ph(NO$_2$)$_2^{\bullet-}$ to $^1$4T*−Ph(NO$_2$) ($k_{-CS}$) were estimated to be $5.1 \times 10^9$, $1.7 \times 10^8$, and $7.5 \times 10^9$ $s^{-1}$, respectively, according to eqs 3−7,[5a,c,11]

$$[^1\text{4T*}-\text{Ph(NO}_2)_2] = C_1\, e^{-\alpha t} + C_2\, e^{-\beta t} \quad (3)$$

$$\alpha = 1/2\{k_{CS} + k_{-CS} + k_0 + k_{CR} + [(-k_{CS} + k_{-CS} - k_0 + k_{CR})^2 + 4k_{CS}k_{-CS}]^{0.5}\} \quad (4)$$

$$\beta = 1/2\{k_{CS} + k_{-CS} + k_0 + k_{CR} - [(-k_{CS} + k_{-CS} - k_0 + k_{CR})^2 + 4k_{CS}k_{-CS}]^{0.5}\} \quad (5)$$

$$C_1 = (k_0 + k_{CS} - \beta)/(\alpha - \beta) \quad (6)$$

$$C_2 = (\alpha - k_0 - k_{CS})/(\alpha - \beta) \quad (7)$$

where $k_0$ is the reciprocal of the $\tau_{fl}$ of **4** in Tol. The ratio of $k_{CS}$ and $k_{-CS}$ was estimated according to $k_{CS}/k_{-CS} = \exp(-\Delta G_{CS}/RT)$.

At 2.6 ns after the laser irradiation, the absorption bands due to $^1$4T*−Ph(NO$_2$)$_2$ and 4T$^{\bullet+}$−Ph(NO$_2$)$_2^{\bullet-}$ disappeared, while the absorption band with a peak at 670 nm remained. From a nanosecond laser flash photolysis, this absorption band was assigned to $^3$4T*−Ph(NO$_2$)$_2$ (vide infra). The $k_{CR}$ of **5** in ANS, THF, and PhCN were estimated to be $1.4 \times 10^{10}$, $2.7 \times 10^{10}$, and $>3.3 \times 10^{10}$ $s^{-1}$, respectively (Figure 5C). In MeCN, the CS and CR processes were not detectable using the picosecond laser flash photolysis, probably due to the faster CS and CR than the present instrumental response. It should be pointed out that the $k_{CR}$ decreased with the increasing solvent polarity, suggesting that the CR processes were in the Marcus inverted region.[3,5,7]

For **4** in ANS and THF, the absorption band of 4T$^{\bullet+}$ was unclear due to the small $\phi_{CS}$ value. In PhCN, the absorption band of 4T$^{\bullet+}$ was clearly observed at 690 nm and rapidly decayed ($k_{CS} > 3.3 \times 10^{10}$ $s^{-1}$). In the case of **4** in MeCN, the CS and CR processes were undetectable as well as for **5** in MeCN. The $k_{CR}$ values of **4** and **5** are summarized in Table 2.

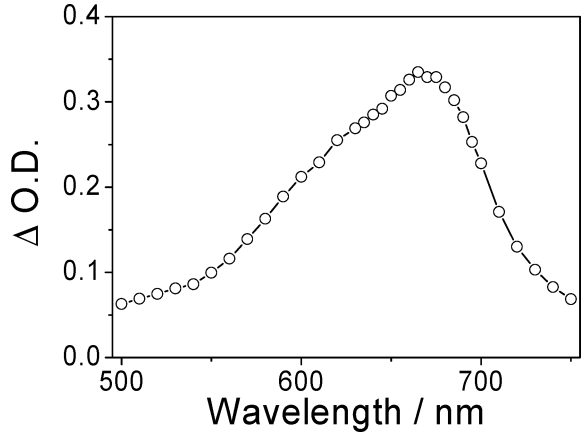


**Figure 6.** Transient absorption spectrum of **5** in Tol at 100 ns during a ns laser flash photolysis employing a ns Nd:YAG laser (355 nm, fwhm 5 ns, 3 mJ pulse$^{-1}$).

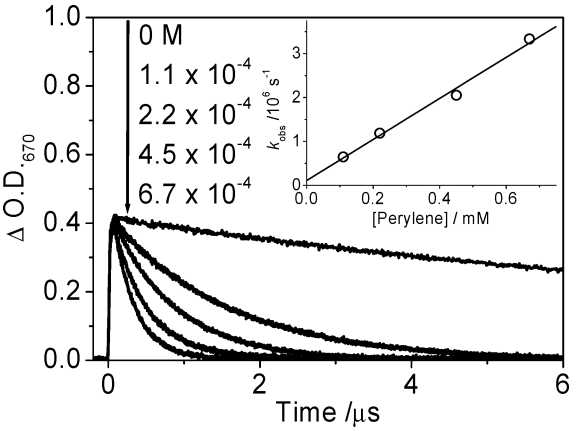


**Figure 7.** Kinetic traces of ΔOD at 670 nm of **4** in benzene in the presence of perylene (0, 0.11, 0.22, 0.45, 0.67 mM) during a ns laser flash photolysis using a XeCl (308 nm, fwhm 40 ns, 3 mJ pulse$^{-1}$) laser. (Inset) Pseudo-first-order plot.

**Nanosecond Laser Flash Photolysis.** Figure 6 shows the transient absorption spectrum of **5** during a nanosecond laser flash photolysis. Because this absorption was effectively quenched by oxygen, the absorption was assigned to $^3$4T*−Ph(NO$_2$)$_2$. The possibility of the assignment of the 4T$^{\bullet+}$ moiety can be ruled out because the near-IR region band specific to 4T$^{\bullet+}$ (1080 nm)[12] was not observed.

In the presence of perylene, a bimolecular energy transfer process from $^3$4T*−PhNO$_2$ to perylene was observed with the rate constant of $5.8 \times 10^9$ M$^{-1}$ s$^{-1}$ in benzene during a 308-nm nanosecond laser irradiation (Figure 7). The extinction coefficient for $^3$4T*−PhNO$_2$ was estimated to be 66 000 M$^{-1}$ cm$^{-1}$ at 670 nm in benzene using perylene as the reference ($^3$perylene*, $\epsilon_{490} = 13\,100$ M$^{-1}$ cm$^{-1}$ in benzene).[14] From the actinometry using benzophenone as the standard (triplet quantum yield ($\phi_T$) = 1, $\epsilon_{530} = 7220$ M$^{-1}$ cm$^{-1}$ in benzene),[14] the $\phi_T$ values were estimated to be 0.38, 0.20, 0.23, 0.10, and 0.11 for **4** in Tol, ANS, THF, PhCN, and MeCN, respectively. For **5**, the $\phi_T$ values were estimated to be 0.35, 0.05, 0.05, 0.05, and 0.04 in Tol, ANS, THF, PhCN, and MeCN, respectively. In the polar solvents, the $\phi_{CS}$ values of **4** and **5** were estimated to be ≥0.99 (Table 2); therefore, $^3$4T*−PhR is considered to be generated from the CR of the CS state with a triplet spin character.[3,15] The photophysical properties of **4** and **5** in the lowest triplet excited states, including the triplet lifetime ($\tau_T$), are summarized in Table 1.

**Energy Diagram.** The first oxidation potentials ($E_{ox}$) of **4** and **5** were evaluated to be 0.69 and 0.70 V versus Ag/AgNO$_3$, respectively, in dichloromethane, which are attributed to the oxidation potentials of the 4T moieties. On the other hand, the reduction potentials ($E_{red}$) of the acceptor moieties in **4** and **5** were −1.34 and −1.10 V, respectively. In the case of $E_{red}$, the half-wave potentials were used because of the irreversible voltammograms. The $-\Delta G_{CS}$ and $-\Delta G_{CR}$ of **4** and **5** were calculated using eqs 8 and 9,[16]

$$-\Delta G_{CR} = -E_{ox} + E_{red} - \Delta Gs \quad (8)$$

$$-\Delta G_{CS} = \Delta E_{0-0} + \Delta G_{CR} \quad (9)$$

where $\Delta G_s$ and $\Delta E_{0-0}$ refer to the solvation energy and the excitation energy of the 4T moiety, respectively. The estimated $\Delta G_{CS}$ and $\Delta G_{CR}$ values are summarized in Table 2.

The energy diagrams of **4** and **5** in Tol and **4** and **5** in polar solvents are summarized in Scheme 1 and Scheme 2, respectively. In these schemes, the position of $^3$4T*−PhR includes some uncertainty. Due to the extended $\pi$-conjugation of the present dyad system, the energy level of $^3$4T*−PhR should be lower than that of $^3$tetrathiophene* (1.83 eV). From the efficient triplet formation after the CS in PhCN and MeCN, the energy level of $^3$4T*−PhR should be lower or similar to that of the CS state in PhCN and MeCN; i.e., the triplet energy of 4T−PhR is lower or similar to $-\Delta G_{CR}$ in PhCN and MeCN (1.43 eV).

In the literature, the reduction potentials of benzene, benzonitrile, phthalonitrile, nitrobenzene, and *m*-dinitrobenzene are reported to be −2.4, −1.9, −1.6, −1.1, and −0.9 V, respectively.[18] Thus, $-\Delta G_{CS}$ should be **1** < **2** < **3** < **4** < **5** in each solvent. In Tol, the CS state is accessible only for **5** while not for the others as indicated in Scheme 1, A and B. In other solvents, the CS state is accessible for **4** and **5** as indicated in Scheme 2. As indicated above, the $k_{CS}$ values of **5** in PhCN and MeCN are almost the same, which can be attributed to the CS around the Marcus top region. Thus, $-\Delta G_{CS} \approx \lambda$ is expected under this condition, i.e., $\lambda \approx 1.0$ eV. According to the semiclassical theory for the intramolecular CS, the $k_{CS}$ value can be estimated according to eq 10,[18]

$$k_{CS} = (4\pi^3/h2\lambda kT)^{1/2}(H_{DA})^2 \exp[-(\Delta G_{CS} + \lambda)^2/4\lambda kT] \quad (10)$$

where $h$ is Planck's constant, $k$ is Boltzmann's constant, $H_{DA}$ is the electronic coupling matrix element, and $T$ is the absolute temperature. The $H_{DA}$ was estimated to be 17 meV for **5** using the $k_{CS} = 5 \times 10^{12}$ s$^{-1}$. The estimated value is rather large, although the center-to-center distance ($R_{CC}$) of the present dyads is rather long (11.7 Å). The estimated value is comparable with the $H_{DA}$ of the dyad, in which the donor and acceptor are directly linked. For example, for the directly linked porphyrin-imide dyads ($R_{CC} \approx 7.2$ Å), the $H_{DA}$ value is reported to be 14 meV.[5b] In this regard, it is considered that the large electronic coupling matrix element of the present dyad can be attributed to the large electronic density of LUMO+1 just below the $^1$4T*−PhR. It should be pointed out that the fast CR process of the present dyad can also be attributed to the existence of a state in which a large electron density localized on the spacer, because such a state enhances the superexchange interaction in the CR process.

## Conclusions

In the present paper, the photoinduced intramolecular CS and CR of tetrathiophene-substituted benzene dyads with an amide spacer were studied. From various fast spectroscopic measure-

**SCHEME 1: Energy Diagrams of 4Aand 5B in Tol**

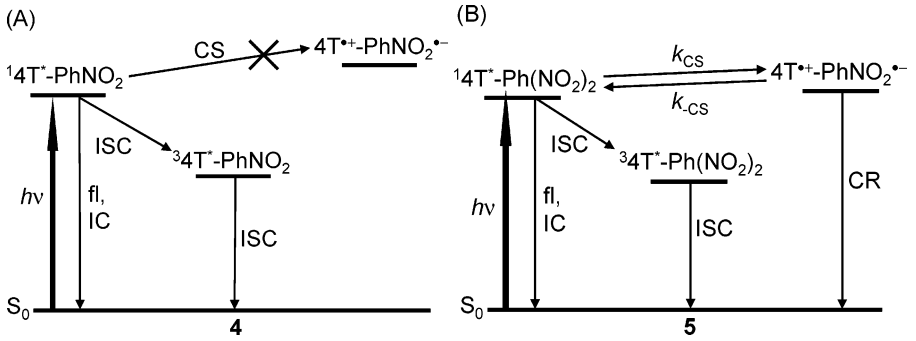


**SCHEME 2: Energy Diagram of 4 and 5 in Polar Solvents**

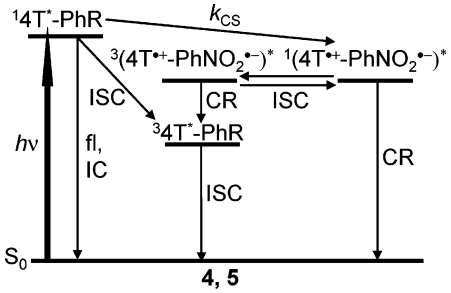


ments, the CS with a rate of $5 \times 10^{12}$ s$^{-1}$ was observed for **5**. The extremely fast CS can be explained by the free energy change of the CS near the Marcus top region and the strong coupling between the donor and acceptor. Furthermore, rather fast CR processes were observed due to the enhanced superexchange interaction through the amide spacer.

## Experimental Section

**Synthesis of the Dyads.** All solvents and reagents were commercially available and used without further purification. The $^1$H NMR spectra of the dyads were recorded using a JEOL JMN EX-270 (270 MHz). The MS spectrometry was performed using a JEOL JMS-600H FAB spectrometer and Shimazu KOMPACT-MALDI PROBE spectrometer, utilizing 3-nitrobenzyl alcohol and 3-hydroxypicolinic acid, respectively.

**3,3‴-Dihexyl-[2,2′;5′,2″;5″,2‴]quaterthiophene-5-carboxylic Acid (4T−COOH).** 4T−COOH was synthesized and purified according to the literature.[19]

**1 (4T−PhH).** The solution of 4T−COOH (84 mg, 0.22 mmol) and $SOCl_2$ (0.21 mL) with a catalytic amount of DMF in benzene (1.6 mL) was stirred for 1 h at room temperature. After the $SOCl_2$ was removed under reduced pressure, the solution of aniline (31 mg, 0.22 mmol) and pyridine (0.01 mL) in benzene (1.8 mL) was dropwise added to the residue in benzene (1.8 mL) and stirred for 3 h at room temperature. The mixture was then extracted with ether (20 mL) and washed with $NaHCO_3$ saturated water (15 mL × 3), and the organic layer was dried over $Na_2SO_4$. After evaporation of the solvent, the residue was purified by silica column and preparative TLC (eluent, 1:1 *n*-hexane−dichloromethane, $R_f = 0.4$) to give the yellow solid. (35 mg, 26%) $^1$H NMR (270 MHz, $CDCl_3$,): $\delta$ 0.89 (m, 6H), 1.32 (m, 12H), 1.62 (m, 4H), 2.67 (t, $J = 7.7$ Hz, 2H), 2.80 (t, $J = 7.7$ Hz, 2H), 6.77 (s, 1H), 6.97 (d, $J = 3.5$ Hz, 1H), 7.16 (m, 4H), 7.37 (t, $J = 8.0$ Hz, 2H), 7.48 (s, 1H), 7.63 (t, $J = 8.0$, 3H); MS (FAB) *m*/*z* 618.

**2 (4T−PhCN).** This compound was obtained in 23% yield in a manner similar to that stated above, using 4-aminobenzonitrile instead of aniline, as an orange solid. $^1$H NMR (270 MHz, $CDCl_3$): $\delta$ 0.86 (m, 6H), 1.29 (m, 12H), 1.61 (m, 4H), 2.64 (m, 4H), 6.77−7.35 (m, 6H), 7.51 (s, 1H), 7.64 (d, 2H), 7.78 (d, 2H), 7.96 (s, 1H); MS (MALDI-TOF) *m*/*z* 643.

**3 (4T−Ph(CN)$_2$).** This compound was obtained in 28% yield in a similar manner as already stated, using 4-aminophthalonitrile instead of aniline, as an orange solid. $^1$H NMR (270 MHz, $CDCl_3$): $\delta$ 0.87 (m, 6H), 1.34 (m, 12H), 1.64 (m, 4H), 2.62 (m, 4H), 6.78−7.37 (m, 6H), 7.54 (s, 1H), 8.00 (m, 2H), 8.23 (d, 1H); MS (MALDI-TOF) *m*/*z* 668.

**4 (4T−PhNO$_2$).** This compound was obtained in 31% yield in a similar manner as already stated, using 4-nitroaniline instead of aniline, as a red solid. $^1$H NMR (270 MHz, $CDCl_3$,): $\delta$ 0.87−0.94 (m, 6H), 1.32−1.37 (m,12H), 2.66−2.82 (m, 4H),1.62−1.68 (m, 4H), 6.94−7.20 (m, 6H), 7.52 (s, 1H), 7.80−7.84 (m, 2H), 7.97 (s, 1H), 8.23−8.26 (m, 2H); MS (FAB) *m*/*z* 664.

**5 (4T−Ph(NO$_2$)$_2$).** This compound was obtained in 38% yield in a similar manner as already stated, using 4-aminophthalonitrile instead of aniline, as a red solid. $^1$H NMR (270 MHz, $CDCl_3$,): $\delta$ 0.87−0.93 (m, 6H), 1.25−1.35 (m, 12H), 1.57−1.75 (m, 4H), 2.69−2.85 (m, 4H), 6.94−7.20 (m, 6H), 7.57 (s, 1H), 8.09 (s, 1H), 8.78−8.79 (t, $J = 2.7$ Hz, 1H), 8.91−8.92 (d, $J = 2.7$ Hz, 2H); MS (FAB) *m*/*z* 708.

**Molecular Orbital Calculations.** All MO calculations were performed at the B3LYP/6-31G(d) level with the Gaussian 03 package.

**Apparatus.** The reduction potentials ($E_{red}$) and oxidation potentials ($E_{ox}$) were measured by cyclic voltammetry on a potentiostat (BAS, CV-50) in a conventional three-electrode cell equipped with a glassy carbon working electrode, a Pt counter electrode, and a $Ag/AgNO_3$ reference electrode at scan rates of 100 mV s$^{-1}$. In each case, the solution containing a 1 mM sample with 0.05 M *n*-$Bu_4NBF_4$ (Aldrich, >99%) was deaerated with argon bubbling.

The steady-state absorption and fluorescence spectra were measured using a Shimadzu UV-3100PC and a Hitachi 850, respectively.

The time-resolved fluorescence measurements in the picosecond to nanosecond time region were carried out by the single-photon counting method using the second harmonic generation (SHG, 430 nm) of a Ti:sapphire laser (Spectra-Physics, Tsunami 3941-M1BB, fwhm 100 fs) as the excitation source. Fluorescence from the sample was detected using a streak camera (Hamamatsu Photonics (4354)) equipped with a polychromator (Acton Research Spectra Pro 150).

The fluorescence lifetime in the subpicosecond regime was estimated using the fluorescence up-conversion method. The SHG (430 nm) of the output of the femtosecond laser (860 nm, 80 fs fwhm, 80 MHz) was used to excite the sample in a cell with a 1.0-mm optical path length. The residual fundamental and the fluorescence were focused in a BBO type I crystal to

generate the sum-frequency oscillation, which was detected by a photomultiplier tube (Hamamatsu Photonics, H8259) and the photon counter (Stanford Research Systems, SR400) after passing through the monochromator (Nikon G250). The cross correlation time of the apparatus was 300 fs fwhm.

The picosecond laser flash photolysis was carried out using the third harmonic oscillation (THG, 355 nm) of a picosecond Nd:YAG laser (Continuum, RGA69-10LD, fwhm 30 ps) as the excitation pulse. The monitoring light was detected with a MOS linear imaging head (Hamamatsu Photonics, M2493-40) equipped with a polychromator (Hamamatsu Photonics, C5094).

For the transient absorption measurements in the microsecond regime, the samples were excited using a THG (355 nm) of a nanosecond Nd:YAG laser (Quantel, Brilliant, fwhm 5 ns) or a XeCl excimer laser (LAMBDA PHYSIK, COMPex 102, 308 nm, fwhm 25 ns).

The pulse radiolysis was performed using an electron pulse (28 MeV, 8 ns, 0.7 kGy) from a L-band linear accelerator at SANKEN, Osaka University.

**Acknowledgment.** This work has been partly supported by a Grant-in-Aid for Scientific Research (Project 17105005, Priority Area (417), 21st Century COE Research, and others) from the Ministry of Education, Culture, Sports, Science, and Technology (MEXT) of Japanese Government.

**Supporting Information Available:** Figure S1, optimized structures and electron densities of the HOMO (A) and LUMO (B) of **1**; Table S1, photophysical properties of **1**, **2**, and **3**. This material is available free of charge via the Internet at http://pubs.acs.org.

## References and Notes

(1) (a) Otsubo, T.; Aso, Y.; Takimiya, K. *J. Mater. Chem.* **2002**, *12*, 2565. (b) Sirringhaus, H.; Brown, P. J.; Friend, R. H.; Nielsen, M. M.; Bechgaard, K.; Langeveld-Voss, B. M. W.; Spiering, A. J. H.; Janssen, R. A. J.; Meijer, E. W.; Herwig, P.; de Leeuw, D. M. *Nature* **1999**, *401*, 685.

(2) (a) Sakai, T.; Satou, T.; Kaikawa, T.; Takimiya, K.; Otsubo, T.; Aso, Y. *J. Am. Chem. Soc.* **2005**, *127*, 8082. (b) Nishinaga, T.; Wakamiya, A.; Yamazaki, D.; Komatsu, K. *J. Am. Chem. Soc.* **2004**, *126*, 3163.

(3) (a) Fujitsuka, M.; Ito, O.; Yamashiro, T.; Aso, Y.; Otsubo, T. *J. Phys. Chem. A* **2000**, *104*, 4876. (b) Fujitsuka, M.; Matsumoto, K.; Ito, O.; Yamashiro, T.; Aso, Y.; Otsubo T. *Res. Chem. Intermed.* **2001**, *27*, 73. (c) Fujitsuka, M.; Masuhara, A.; Kasai, H.; Oikawa, H.; Nakanishi, H.; Ito, O.; Yamashiro, T.; Aso, Y.; Otsubo, T. *J. Phys. Chem. B* **2001**, *105*, 9930. (d) Araki, Y.; Luo, H.; Nakamura, T.; Fujitsuka, M.; Ito, O.; Kanato, H.; Aso, Y.; Otsubo, T. *J. Phys. Chem. A* **2004**, *108*, 10649. (e) Beek, W. J. E.; Janssen, R. A. J. *J. Mater. Chem.* **2004**, *14*, 2795.

(4) Nakamura, T.; Fujitsuka, M.; Araki, Y.; Ito, O.; Ikemoto, J.; Takimiya, K.; Aso, Y.; Otsubo, T. *J. Phys. Chem. B* **2004**, *108*, 10700. (b) Kanato, H.; Takimiya, K.; Aso, Y.; Nakamura, T.; Araki, Y.; Ito, O. *J. Org. Chem.* **2004**, *69*, 7183. (c) Yamanaka, K.; Fujitsuka, M.; Araki, Y.; Ito, O.; Aoshima, T.; Fukushima, T.; Miyashi, T. *J. Phys. Chem. A* **2004**, *108*, 250. (d) Odobel, F.; Suresh, S.; Blart, E.; Nicolas, Y.; Quintard, J.; Janvier, P.; Questel, J. L.; Illien, B.; Rondeau, D.; Richomme, P.; Häupl, T.; Wallin, S.; Hammarström, L. *Chem.*−*Eur. J.* **2002**, *8*, 3027. (e) Ikemoto, J.; Takimiya, K.; Aso, Y.; Otsubo, T.; Fujitsuka, M.; Ito, O. *Org. Lett.* **2002**, *4*, 309. (f) van Hal, P. A.; Knol, J.; Langeveld-Voss, B. M. W.; Meskers, S. C. J.; Hummelen, J. C.; Janssen, R. A. J. *Synth. Met.* **2001**, *116*, 123. (g) van Hal, P. A.; Janssen, R. A. J.; Lanzani, G.; Gerullo, G.; ZavelaniRossi, M.; De Silvestri, S. *Chem. Phys. Lett.* **2001**, *345*, 33. (h) van Hal, P. A.; Knol, J.; Langeveld-Voss, B. M. W.; Meskers, S. C. J.; Hummelen, J. C.; Janssen, R. A. J. *J. Phys. Chem. A* **2000**, *104*, 5974. (i) Würthner, F.; Vollmer, M. S.; Effenberger, F.; Emele, P.; Meyer, D. U.; Port, H.; Wolf, H. C. *J. Am. Chem. Soc.* **1995**, *117*, 8090.

(5) (a) Mataga, N.; Taniguchi, S.; Chosrowjan, H.; Osuka, A.; Kurotobi, K. *Chem. Phys. Lett.* **2005**, *403*, 163. (b) Yoshida, N.; Ishizuka, T.; Yofu, K.; Murakami, M.; Miyasaka, H.; Okada, T.; Nagata, Y.; Itaya, A.; Cho, H. S.; Kim, D.; Osuka, A. *Chem.*−*Eur. J.* **2003**, *9*, 2854. (c) Mataga, N.; Taniguchi, S.; Chosrowjan, H.; Osuka, A.; Yoshida, N. *Chem. Phys.* **2003**, *295*, 215. (d) Mataga, N.; Chosrowjan, H.; Taniguchi, S.; Shibata, Y.; Yoshida, N.; Osuka, A.; Kikuzaw, T.; Okada, T. *J. Phys. Chem. A* **2002**, *106*, 12191. (e) Mataga, N.; Chosrowjan, H.; Shibata, Y.; Yoshida, N.; Osuka, A.; Kikuzawa, T.; Okada, T. *J. Am. Chem. Soc.* **2001**, *123*, 12422. (f) Macpherson, A. N.; Liddell, P. A.; Lin, S.; Noss, L.; Seely, G. R.; DeGraziano, J. M.; Moore, A. L.; Moore, T. A.; Gust, D. *J. Am. Chem. Soc.* **1995**, *117*, 7202. (g) Beckers, E. H. A.; Meskers, S. C. J.; Schenning, A. P. H. J.; Chen, Z.; Würthner, F.; Janssen, R. A. J. *J. Phys. Chem. A* **2004**, *108*, 6933.

(6) (a) de Silva, A. P.; Gunaratne, H. Q. N.; Gunnlaugsson, T.; Huxley, A. J. M.; McCoy, C. P.; Rice, T. E. *Chem. Rev.* **1997**, *97*, 1515. (b) Collier, C. P.; Matterstei, G.; Wong, E. W.; Luo, Y.; Beverly, K.; Sampaio, J.; Raymo, F. M.; Stoddart, J. F.; Heath, J. R. *Science*, **2000**, *289*, 1172. (c) de Silva, A. P.; Gunaratne, H. Q. N.; McCoy, C. P. *Nature*, **1993**, *364*, 42. (d) Lukas, A. S.; Bushard, P. J.; Wasielewski, M. R. *J. Am. Chem. Soc.* **2001**, *123*, 2440.

(7) Marcus, R. A. *J. Chem. Phys.* **1956**, *24*, 966.

(8) Fukuzumi, S.; Yoshida, Y.; Okamoto, K.; Imahori, H.; Araki, Y.; Ito, O. *J. Am. Chem. Soc.* **2002**, *124*, 6794.

(9) (a) McConnell, H. M. *J. Chem. Phys.* **1961**, *35*, 508. (b) Bavis, W. B.; Svec, W. A.; Ratner, M. A.; Wasielewski, M. R. *Nature* **1998**, *396*, 60. (c) Lukas, A. S.; Bushard, P. J.; Wasielewski, M. R. *J. Am. Chem. Soc.* **2001**, *123*, 2440. (d) Goldsmith, R. H.; Sinks, L. E.; Kelley, R. F.; Betzen, L. J.; Liu, W.; Weiss, E. A.; Ratner, M. A.; Wasielewski, M. R. *Proc. Natl. Acad. Sci. U.S.A.* **2005**, *102*, 3540.

(10) Becker, R. S.; de Melo, J. S.; Macanita, A. L.; Elisei, F. *J. Phys. Chem.* **1996**, *100*, 18683.

(11) (a) Osuka, A.; Marumo, S.; Mataga, N.; Taniguchi, S.; Okada, T.; Yamazaki, I.; Nishimura, Y.; Ohno, T.; Nozaki, K *J. Am. Chem. Soc.* **1996**, *118*, 155. (b) Asahi, T.; Ohkohchi, M.; Matsusaka, R.; Mataga, N.; Zhang, R. P.; Osuka, A.; Maruyama, K. *J. Am. Chem. Soc.* **1993**, *115*, 5665. (c) Gaines, G. L.; O'Neil, M. P.; Svec, W. A.; Niemczyk, M. P.; Wasielewski, M. R. *J. Am. Chem. Soc.* **1991**, *113*, 719. (d) Heitele, H.; Finckh, P.; Pöllinger, F.; Michel-Beyerle, M. E. *J. Phys. Chem.* **1989**, *93*, 5173.

(12) Matsumoto, K.; Fujitsuka, M.; Sato, T.; Onodera, S.; Ito, O. *J. Phys. Chem. B* **2000**, *104*, 11632.

(13) Samori, S.; Hara, M.; Tojo, S.; Fujitsuka, M.; Yang, S.; Elangovan, A.; Ho, T.; Majima, T. *J. Phys. Chem. B* **2005**, *109*, 11735.

(14) Murov, S. L.; Carmichael, I.; Hug, G. L. *Handbook of Photochemistry*; Marcel Dekker: New York, 1993.

(15) (a) Weiss, E. A.; Tauber, M. J.; Ratner, M. A.; Wasielewski, M. R. *J. Am. Chem. Soc.* **2005**, *127*, 6052. (b) Sinks, L. E.; Weiss, E. A.; Giaimo, J. M.; Wasielewski, M. R. *Chem. Phys. Lett.* **2005**, *404*, 244. (c) Weiss, E. A.; Ahrens, M. J.; Sinks, L. E.; Ratner, M. A.; Wasielewski, M. R. *J. Am. Chem. Soc.* **2004**, *126*, 9510. (d) Weiss, E. A.; Chernick, E. T.; Wasielewski, M. R. *J. Am. Chem. Soc.* **2004**, *126*, 2326. (e) Shaakov, S.; Galili, T.; Stavitski, E.; Levanon, H.; Lukas, A.; Wasielewski, M. R. *J. Am. Chem. Soc.* **2003**, *125*, 6563. (f) Lukas, A. S.; Bushard, P. J.; Weiss, E. A.; Wasielewski, M. R. *J. Am. Chem. Soc.* **2003**, *125*, 3921. (g) Weiss, E. A.; Ratner, M. A.; Wasielewski, M. R. *J. Phys. Chem. A* **2003**, *107*, 3639. (h) Kobori, Y.; Sekiguchi, S.; Akiyama, K.; Tero-Kubota, S. *J. Phys. Chem. A* **1999**, *103*, 5416.

(16) Rehm, D.; Weller, A. *Isr. J. Chem.* **1970**, *8*, 259. (b) Weller, A. Z. *Phys. Chem. Neue Folge* **1982**, *133*, 93.

(17) Reed, R. C.; Wightman, R. M. In *Encyclopedia of Electrochemistry of the Elements*; Bard, A. J., Ed.; Marcel Dekker: New York, 1984.

(18) Marcus, R. A.; Sutin, N. *Biochim. Biophys. Acta* **1985**, *811*, 265.

(19) Higuchi, H.; Uraki, Y.; Yokota, H.; Koyama, H.; Ojima, J.; Wada, T.; Sasabe, H. *Bull. Chem. Soc. Jpn.* **1998**, *71*, 483.